SLAC-PUB-12118
Revised - July 2007
astro-ph/0609274

Super-critically accreting stellar-mass black holes as ultraluminous X-ray sources

Juri Poutanen,[1,2⋆] Galina Lipunova,[3] Sergei Fabrika,[4⋆] Alexey G. Butkevich[1,5] and Pavel Abolmasov[4]

[1]*Astronomy Division, P.O. Box 3000, 90014 University of Oulu, Finland*
[2]*KIPAC, Stanford University P.O. Box 20450, MS29, Stanford, CA 94309, USA*
[3]*Sternberg Astronomical Institute, Moscow State University, Universitetskij pr. 13, 119992 Moscow, Russia*
[4]*Special Astrophysical Observatory, 369167 Nizhnij Arkhyz, Karachaevo-Cherkesiya, Russia*
[5]*Pulkovo Observatory, Pulkovskoye shosse 65, 196140 Saint-Petersburg, Russia*

ABSTRACT

We derive the luminosity-temperature relation for the super-critically accreting black holes (BHs) and compare it to the data on ultraluminous X-ray sources (ULXs). At super-Eddington accretion rates, an outflow forms within the spherization radius. We construct the accretion disc model accounting for the advection and the outflow, and compute characteristic disc temperatures. The bolometric luminosity exceeds the Eddington luminosity $L_{\rm Edd}$ by a logarithmic factor $1+0.6\ln\dot{m}$ (where $\dot{m}$ is the accretion rate in Eddington units) and the wind kinetic luminosity is close to $L_{\rm Edd}$. The apparent luminosity for the face-on observer is 2–7 times higher because of geometrical beaming. Such an observer has a direct view of the inner hot accretion disc, which has a peak temperature $T_{\rm max}$ of a few keV in stellar-mass BHs. The emitted spectrum extends as a power-law $F_E\propto E^{-1}$ down to the temperature at the spherization radius $T_{\rm sp}\approx\dot{m}^{-1/2}$ keV. We associate $T_{\rm max}$ with a few keV spectral components and $T_{\rm sp}$ with the soft, 0.1–0.2 keV components observed in ULXs. An edge-on observer sees only the soft emission from the extended envelope, with the photosphere radius exceeding the spherization radius by orders of magnitude. The dependence of the photosphere temperature on luminosity is consistent with that observed in the super-Eddington accreting BHs SS 433 and V4641 Sgr. Strong outflows combined with the large intrinsic X-ray luminosity of the central BH explain naturally the presence of the photoionized nebulae around ULXs. An excellent agreement between the model and the observational data strongly argues in favour of ULXs being super-critically accreting, stellar-mass BHs similar to SS 433, but viewed close to the symmetry axis.

Key words: accretion, accretion discs – black holes physics – X-ray: binaries – X-ray: galaxies

1 INTRODUCTION

A large number of ultraluminous X-ray sources (ULXs) has been discovered in the nearby star-forming galaxies (see Mushotzky 2004, for a review). Their luminosities exceed considerably $2\times10^{39}{\rm erg\ s^{-1}}$, the Eddington limit for a stellar-mass ($\sim10{\rm M}_\odot$) black hole (BH). This was argued to be the evidence for existence of the intermediate-mass BHs (IMBHs, with $M=10^2$–$10^4{\rm M}_\odot$; Colbert & Mushotzky 1999). The large apparent luminosities can also be produced by super-critical accretion on to a stellar-mass BH (Shakura & Sunyaev 1973, hereafter SS73; Jaroszyński et al. 1980; Abramowicz et al. 1988; Lipunova 1999; Fabrika 2004; Begelman et al. 2006), or by the geometric (Fabrika & Mescheryakov 2001; King et al. 2001) or relativistic (Reynolds et al. 1997; Körding et al. 2002) collimation of radiation.

A strong argument in favour of IMBHs is the presence of a soft, 0.1–0.2 keV component in their spectra (Kaaret et al. 2003; Miller et al. 2003, 2004). Arguments against the IMBH interpretation include theoretical problems with their formation (King et al. 2001) and their non-standard spectra, which show a cutoff at a few keV (Stobbart et al. 2006), while other BHs, stellar as well as super-massive, at a few per cent of Eddington luminosity have hard power-law-like spectra (Zdziarski et al. 1997). Furthermore, the observed anti-correlation between luminosity and temperature contradicts the $L\propto T^4$ law expected for standard accretion discs (Feng & Kaaret 2007) and some ULXs show a harder, 1–4 keV

⋆ E-mail: juri.poutanen@oulu.fi (JP); galja@sai.msu.ru (GL); fabrika@sao.ru (SF)

Submitted to Mon.Not.Roy.Astron.Soc.

Work supported in part by US Department of Energy contract DE-AC02-76SF00515

thermal component with the corresponding radius of only 30–40 km (Makishima et al. 2000; Stobbart et al. 2006). All this raises further doubts on the IMBH interpretation. The soft components can be interpreted as signatures of an extended photosphere (SS73; Lipunova 1999; King & Pounds 2003), but then we need to explain the simultaneous presence of the harder emission.

The low-frequency, 0.02–0.2 Hz, quasi-periodic oscillations detected from ULXs in M82 (Strohmayer & Mushotzky 2003), Holmberg IX (Dewangan et al. 2006), and NGC 5408 (Strohmayer et al. 2007), if interpreted as the Keplerian frequencies at the innermost stable orbit around a BH, argue in favour of IMBHs. However, oscillations with very similar frequencies have been observed from the BHs in the Milky Way, Cygnus X-1 (Vikhlinin et al. 1994) and GRS 1915+105 (Morgan et al. 1997), which certainly are not IMBHs.

Important clues on the nature of ULXs come from the presence of extended photoionized nebulae around them (Wang 2002; Pakull & Mirioni 2003; Kaaret et al. 2004). The observations imply a rather isotropic source of the ionizing radiation rejecting the idea of a strong beaming of radiation. The nebulae are dynamically perturbed with the velocity gradients of $\sim$ 50–100 km s^{-1} on the scale of 50–100 pc (Lehmann et al. 2005; Fabrika & Abolmasov 2006; Ramsey et al. 2006). This points towards the activity of the central engine in form of a wind or a jet. The ULX nebulae are similar to W50, the nebulae around SS 433, the only known persistent supercritical accretor in the Milky Way, radiating presumably around 10^{40}erg s^{-1} in the UV (Dolan et al. 1997). A super-critically accreting compact source can produce strong winds and jets which can inflate the nebulae (Begelman et al. 1980; Lehmann et al. 2005; Pakull et al. 2006; Fabrika & Abolmasov 2006; Abolmasov et al. 2007). On the other hand, there is no good physical reason why a sub-critically accreting IMBH would produce such a strong outflow.

The observed similarities between W50 and ULX nebulae lead us to consider seriously the idea that the central engines of ULXs are super-critically accreting stellar mass BHs similar to SS 433. We do not see directly the X-ray source in SS 433, but if observed along the symmetry axis, it would be a bright X-ray source (Katz 1986), which we interpret as an ULX (Fabrika & Mescheryakov 2001; King 2002; Fabrika 2004; Begelman et al. 2006).

In this paper, we develop a model for the super-critical accretion disc accounting for the effects of advection and outflows. We also construct a one-dimensional, vertically integrated model of the wind, estimate the optical depth through the wind and determine characteristic temperatures as a function of the mass accretion rate and the luminosity. We further compare the resulting luminosity-temperature relations to the data on ULXs as well as the BHs in our galaxy and LMC.

2 SUBCRITICAL ACCRETION DISCS

The standard accretion disc theory (SS73) can be applied when the accretion rate is not very high and the luminosity does not exceed the Eddington limit

$$L_{\rm Edd}=\frac{GM\dot{M}_{\rm Edd}}{2R_{\rm in}}=\frac{4\pi GMc}{\kappa}=1.5\,10^{38}\,m\frac{1.7}{1+X}\,{\rm erg\,s^{-1}}, \quad (1)$$

where $\dot{M}_{\rm Edd}=48\pi GM/c\kappa=2\ 10^{18}m$ g s^{-1} is the Eddington accretion rate, $R_{\rm in}=3R_{\rm S}$ is the inner disc radius, $R_{\rm S}=2GM/c^2$ is the Schwarzschild radius. The stellar mass, measured in solar masses, is $m=M/{\rm M}_\odot$, $\kappa=0.2(1+X)=0.34$ cm^2 g^{-1} is the Thomson opacity and X is the hydrogen mass fraction (which we assume equal to solar $X=0.7$).

The energy flux from one face of the disc (in Newtonian approximation) as a function of radius R is

$$Q^+(R)=\frac{3}{8\pi}\frac{GM\dot{M}}{R^3}\left[1-r^{-1/2}\right], \quad (2)$$

where $\dot{M}$ is the accretion rate and $r=R/R_{\rm in}$. This results in the effective temperature variation $T(R)\propto R^{-3/4}$ at large R and the maximum observed color temperature

$$T_{\rm c,max}=1.26f_{\rm c}\,m^{-1/4}\dot{m}^{1/4}\ {\rm keV}, \quad (3)$$

which is reached at $r_{\rm max}=(3/2)^{4/5}\approx 1.38$. Here $\dot{m}=\dot{M}/\dot{M}_{\rm Edd}$ is dimensionless accretion rate. The color correction $f_{\rm c}\approx 1.7$ (e.g. Shimura & Takahara 1995) describes the hardening of the spectrum relative to the black body. The emitted flux $F_E\propto E^{1/3}$ at $E\lesssim kT_{\rm c,max}$. The total emitted luminosity,

$$L=\int_{R_{\rm in}}^{\infty}Q^+(R)4\pi R{\rm d}R=\dot{m}L_{\rm Edd}, \quad (4)$$

depends on the maximum temperature as $L\propto T_{\rm c,max}^4$.

3 SUPERCRITICAL ACCRETION DISCS

The matter supply to the BH in a close binary can significantly exceed the Eddington rate, $\dot{m}_0=\dot{M}_0/\dot{M}_{\rm Edd}\gg 1$. There are two different views on the way the accretion proceeds in this regime.

(i) The 'Polish doughnut' or slim disc models (Jaroszyński et al. 1980; Abramowicz et al. 1988) assume that all the supplied gas reaches the BH, but most of the gravitational energy released in the disc is advected into the hole as the photons are trapped in the flow. Inside the trapping radius $R_{\rm tr}$ (where photon diffusion and accretion time-scale are equal), the vertical component of gravity scales as R^{-2} (as the disc relative scale-height H/R is of the order unity) resulting in the same radial dependence of the radiation flux $Q_{\rm rad}$, because the disc is radiation pressure supported. This implies the effective temperature distribution $R^{-1/2}$ and a flat (in EF_E) emitted spectrum $F_E\propto E^{-1}$ (see e.g. Watarai et al. 2000). Naturally, a logarithmic dependence of bolometric luminosity of inner supercritical disc on $\dot{M}_0$ is yielded:

$$L\propto\int\limits_{R_{\rm in}}^{R_{\rm tr}}Q_{\rm rad}(R)R\,{\rm d}R\propto\int\limits_{R_{\rm in}}^{R_{\rm tr}}R^{-1}{\rm d}R=\ln\left(\frac{R_{\rm tr}}{R_{\rm in}}\right)\approx\ln\dot{m}_0. \quad (5)$$

The last relation follows from the fact that the trapping radius scales with the accretion rate as $R_{\rm tr}\approx\dot{m}_0R_{\rm in}\gg R_{\rm in}$. The total disc luminosity exceeds the Eddington one by a logarithmic factor:

$$L_{\rm bol}\approx L_{\rm Edd}\,(1+\ln\dot{m}_0). \quad (6)$$

(ii) Alternatively, instead of spending most of the dissipated energy to increase the entropy of the gas, this energy can be spent to eject the excess mass (SS73). In this model most of the gas is blown away by the radiation pressure, the accretion rate decreased linearly with radius $\dot{M}(R)\propto R$, and only a small fraction of it, $\dot{m}\sim 1$, makes it to the hole.[1] The linear dependence of the accretion rate

[1] A similar physics might operate at a very low accretion rate, when the gas cannot cool resulting in a positive Bernoulli parameter. This implies that the gas is effectively unbound and can easily produce outflows (Narayan & Yi 1994; Blandford & Begelman 1999).

on radius results in the R^{-2} dependence of the radiative flux.[2] The luminosity and the disc effective temperature radial distribution are very similar to the slim disc case (see below). The largest difference is in the presence of a strong wind which blocks and reprocesses the radiation from the central part of the disc. The observed spectrum, therefore, depends on the velocity structure and geometry of the wind and the position of the observer relative to the disc rotational axis.

Reality might be somewhere in between, with both advection and outflow operating together as shown by the numerical simulations (Eggum et al. 1988; Ohsuga et al. 2005; Okuda et al. 2005). Below we first construct a one-dimensional, vertically integrated model of the supercritical disc with the outflow and then discuss the effect of the wind on the emergent spectrum.

3.1 Supercritical disc with outflow and without advection

The scale-height of accretion discs for $\dot{m}_0 \sim 1$ is determined by the balance between the radiation pressure force and the vertical component of gravity (SS73),

$$\frac{H}{R} = \dot{m}_0 \frac{3}{r}\left[1 - r^{-1/2}\right]. \tag{7}$$

When the accretion rate exceeds the critical value $\dot{m}_{\rm cr} = 9/4$, the ratio H/R exceeds unity at some radii and the outflow is inevitable. Accurate calculations (Bisnovatyi-Kogan & Blinnikov 1977) show that the outflow can start even at a smaller rate. At $\dot{m}_0 \gg \dot{m}_{\rm cr}$, the disc starts 'feeling' that it is supercritical at the spherization radius $r_{\rm sp} = R_{\rm sp}/R_{\rm in} \approx \dot{m}_0$, where the outflow starts.

The wind affects the disc structure by removing the angular momentum. The modified angular momentum conservation equation is (see e.g. Lipunova 1999)

$$\frac{\mathrm{d}}{\mathrm{d}R}\left(\dot{M}(R)\omega_{\rm K}R^2\right) = \frac{\mathrm{d}g(R)}{\mathrm{d}R} + \omega_{\rm K}R^2\frac{\mathrm{d}\dot{M}(R)}{\mathrm{d}R}, \tag{8}$$

where $\omega_{\rm K}(R) = (GM/R^3)^{1/2}$ is the Keplerian angular velocity,

$$g(R) = 2\pi\, T_{r\phi}R^2 \tag{9}$$

is the torque and $T_{r\phi} = 2H\, t_{r\phi}$ is the vertically integrated viscous stress. The first term on the right hand side of equation (8) is responsible for transfer of the angular momentum by viscosity, while the second term is the momentum transfer by the outflowing matter. The viscous heating rate per unit area is

$$2Q^+(R) = -T_{r\phi}R\frac{\mathrm{d}\omega_{\rm K}}{\mathrm{d}R} = \frac{3}{2}T_{r\phi}\omega_{\rm K} = \frac{3}{4\pi}\omega_{\rm K}\frac{g(R)}{R^2}. \tag{10}$$

If advection is not accounted for, all dissipated energy is converted locally to the radiation:

$$Q^+(R) = Q_{\rm rad}(R). \tag{11}$$

We can assume that a fraction $\epsilon_{\rm w}$ of the radiative energy goes to accelerate the outflow:

$$\epsilon_{\rm w}Q_{\rm rad}(R) = \frac{1}{2}\frac{1}{2\pi R}\frac{\mathrm{d}\dot{M}(R)}{\mathrm{d}R}\frac{\omega_{\rm K}^2R^2}{2} = \frac{GM}{8\pi R^2}\frac{\mathrm{d}\dot{M}(R)}{\mathrm{d}R}. \tag{12}$$

where $v_{\rm K}^2(R)/2 = \omega_{\rm K}^2R^2/2$ is the energy required to eject a unit mass from radius R to infinity. Lipunova (1999) assumed the maximum outflow rate with $\epsilon_{\rm w} = 1$ and obtained an analytical solution of the system of equations (8)–(12), applying boundary conditions $\dot{M}(R_{\rm sp}) = \dot{M}_0$ (where $R_{\rm sp}$ is a parameter of the model) and $g(R_{\rm in}) = 0$:

$$\frac{\dot{M}(r)}{\dot{M}_{\rm Edd}} = \begin{cases} \dot{m}_0\dfrac{r}{r_{\rm sp}}\dfrac{1+\frac{2}{3}r^{-5/2}}{1+\frac{2}{3}r_{\rm sp}^{-5/2}}, & r \le r_{\rm sp}, \\ \dot{m}_0, & r > r_{\rm sp}, \end{cases} \tag{13}$$

$$\frac{g(r)}{g_0} = \begin{cases} \dfrac{\dot{m}_0 r^{3/2}}{3r_{\rm sp}}\dfrac{1-r^{-5/2}}{1+\frac{2}{3}r_{\rm sp}^{-5/2}}, & r \le r_{\rm sp}, \\ \dfrac{g(r_{\rm sp})}{g_0} + \dot{m}_0\left(r^{1/2} - {r_{\rm sp}}^{1/2}\right), & r > r_{\rm sp}. \end{cases} \tag{14}$$

where $g_0 = \dot{M}_{\rm Edd}\sqrt{GMR_{\rm in}}$.

At intermediate radii $1 \ll r < r_{\rm sp}$, the accretion rate is close to the dependence $\dot{M}(r) = \dot{M}_0\, r/r_{\rm sp}$ suggested by SS73 and the radiative energy flux is

$$Q_{\rm rad}(R) = \frac{3}{8\pi}\frac{(GM)^{1/2}g(r)}{R^{7/2}} \approx \frac{GM\dot{M}(R)}{8\pi\, R^3} \propto R^{-2}. \tag{15}$$

Note that in the standard model there is a factor of 3 present in a similar formula (see equation 2), which is related to the fact that the energy dissipated close to the inner disc radius is transported to larger radii and radiated there. In the model with the mass loss, this factor is missing, implying that the energy transfer from the inner part of the disc is negligible.

The luminosities produced within and outside $r_{\rm sp}$ are

$$\begin{aligned} \frac{L(r<r_{\rm sp})}{L_{\rm Edd}} &= \frac{\dot{m}_0}{r_{\rm sp}}\frac{\ln r_{\rm sp} - \frac{2}{5}\left(1 - r_{\rm sp}^{-5/2}\right)}{1+\frac{2}{3}r_{\rm sp}^{-5/2}}, \\ \frac{L(r>r_{\rm sp})}{L_{\rm Edd}} &= \frac{5}{3}\frac{\dot{m}_0}{r_{\rm sp}}\frac{1}{1+\frac{2}{3}r_{\rm sp}^{-5/2}}. \end{aligned} \tag{16}$$

Defining the spherization radius by the condition (SS73)

$$L(r > r_{\rm sp}) = L_{\rm Edd}, \tag{17}$$

we obtain

$$r_{\rm sp} \approx \frac{5}{3}\,\dot{m}_0, \tag{18}$$

which gives the total luminosity

$$L \approx L_{\rm Edd}\left(1 + \frac{3}{5}\ln\dot{m}_0\right) \tag{19}$$

and the Eddington accretion rate to the BH, $\dot{m}(R_{\rm in}) = 1$. A fraction of this luminosity can escape as radiation and the rest as kinetic energy of the outflow.

It is worth noting here that if we assume in this model that only a small fraction of the dissipated energy is used to produce the outflow, i.e. $\epsilon_{\rm w} < 1$ (see eq. 12), then the resulting accretion rate is too high. With the high radiative efficiency (because we neglect advection) the locally emitted flux is strongly super-Eddington, and therefore the model is unphysical. However, accounting for the advection allows us to construct a self-consistent model even in this case (see below).

3.2 Supercritical disc with advection

At supercritical accretion rates, the advective transport of the viscously generated heat to the black hole becomes important in the

[2] We note here that any supercritical disc model (with advection, with outflows, or both) predicts such a dependence, which just follows from the vertical balance of gravity and radiative pressure.

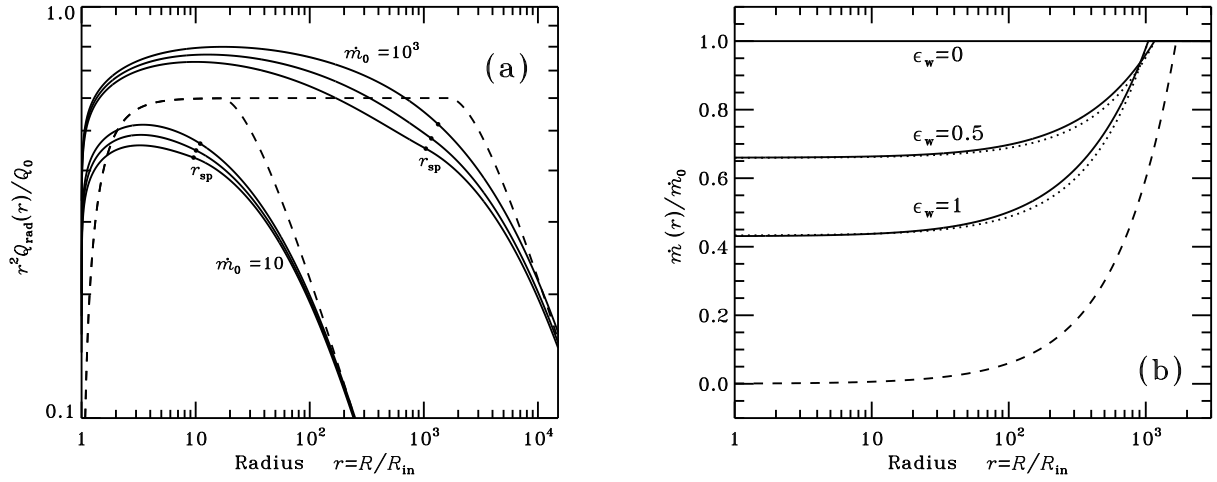

Figure 1. (a) The radiative energy flux emitted from the disc (times r^2, i.e. energy flux per logarithm of radius) as a function of radius for $\dot{m}_0 = 10$ and 10^3. The flux is measured in units $Q_0 = GM\dot{M}_{\rm Edd}/8\pi R_{\rm in}^3 = c^5/36GM\kappa = 1.52\,10^{25} m^{-1}$erg cm^{-2} s^{-1}. The solid curves from the top to the bottom are the exact solutions of the advective disc equations for $\epsilon_{\rm w} = 0, 1/2$ and 1. Bold dots represent the positions of the spherization radius defined by condition (17). The dashed curves correspond to the analytical solution given by equations (10), (11) and (14). (b) The accretion rate as a function of radius for $\dot{m}_0 = 10^3$. The solid curves are the exact solutions for the advective disc, while the dashed curve is solution (13) for the non-advective disc with the outflow. The dotted curves are the linear approximations given by formula (25).

energy balance equation. The diffusion time for photons, traveling to the disc surface, becomes larger than the characteristic time of the radial displacement of the matter. Due to the advective removing of the heat, the locally radiated flux becomes smaller:

$$Q_{\rm rad} = Q^+ - Q_{\rm adv}\,. \tag{20}$$

A model of a supercritical advective disc with an outflow was first proposed by Lipunova (1999) (see also Kitabatake, Fukue & Matsumoto 2002; Fukue 2004). The maximum mass loss from an advective disc by the energy-driven wind is about twice smaller than in the model without advection and amounts to about 3/5 of initial accretion rate $\dot{M}_0$. We modify the model considered by Lipunova (1999) assuming that a fraction $\epsilon_{\rm w} < 1$ of the radiation energy flux is spent on the production of the outflow (see eq. [12]). We solve the standard set of equations for the advective disc (as described in details in Lipunova 1999) for various $\dot{m}_0$ and $\epsilon_{\rm w}$.

The outflow occurs within the spherization radius $r_{\rm sp}$, which is defined self-consistently from condition (17). For different $\epsilon_{\rm w}$, the spherization radius varies because a different amount of angular momentum is gone with the wind, and, consequently, the structure of the outer subcritical disc is different as it depends on the boundary condition at $r_{\rm sp}$. The results of our calculations can be approximated (with the accuracy of 2 per cent for $\dot{m}_0 > 5$) by a simple formula:

$$\frac{r_{\rm sp}}{\dot{m}_0} \approx 1.34 - 0.4\epsilon_{\rm w} + 0.1\epsilon_{\rm w}^2 - (1.1 - 0.7\epsilon_{\rm w})\dot{m}_0^{-2/3}. \tag{21}$$

The resulting radiation flux and the mass accretion rate as functions of radius are shown in Fig. 1. One sees that the radiative energy flux depends very weakly on $\epsilon_{\rm w}$. This also means that a similar solution will be obtained if a smaller mass is ejected with a larger velocity. The radial dependence of $Q_{\rm rad}(r)$ is similar to that in discs with strong mass loss and no advection (see section 3.1 and the dashed curve in Fig. 1a). At $r < r_{\rm sp} \approx \dot{m}_0$, $Q_{\rm rad}(r)r^2$ is almost constant. This is just the consequence of the fact that the disc is close to the Eddington limit locally everywhere, i.e. H/R is close to unity. At $r \gg r_{\rm sp}$, $Q_{\rm rad}$ decreases as r^{-3} as in the standard disc. The total luminosity is well approximated by equation (19). As we assume that a fraction $\epsilon_{\rm w} < 1$ of the radiative energy flux is spent to drive the wind to infinity, a fraction $1 - \epsilon_{\rm w}$ can escape as radiation. We note that in the advective disc (with or without the outflow) the scale-height (see Beloborodov 1998; Lipunova 1999, and Fig. 1a)

$$H/R \approx \frac{r^2\,Q_{\rm rad}(r)}{Q_0} < 0.8, \tag{22}$$

which justifies our use of the vertically integrated quantities.

Because the outflow is optically thick at most radii and the radiation is partially trapped (see below), it is *energy-driven* (not *momentum-driven* as was assumed by King & Pounds 2003), and its kinetic luminosity can exceed $L_{\rm Edd}$.

The fraction of the initial accretion rate that passes through the inner radius can be approximated for $\dot{m}_0 > 2.5$ as

$$\frac{\dot{m}_{\rm in}}{\dot{m}_0} \approx \frac{1-a}{1 - a\left(\frac{2}{5}\dot{m}_0\right)^{-1/2}}, \tag{23}$$

where $a = \epsilon_{\rm w}(0.83 - 0.25\epsilon_{\rm w})$. For example, for $\dot{m}_0 = 1000$ and $\epsilon_{\rm w} = 1/2$ we get $r_{\rm sp} = 1.16\,\dot{m}_0$ and $\dot{m}_{\rm in} = 0.66\,\dot{m}_0$, while in the case of the maximal outflow with $\epsilon_{\rm w} = 1$ we have $r_{\rm sp} = 1.04\,\dot{m}_0$ and $\dot{m}_{\rm in} = 0.43\,\dot{m}_0$. The total outflow rate for large $\dot{m}_0$ is thus

$$\dot{M}_{\rm w} \approx a\dot{M}_0. \tag{24}$$

The exact solutions for the accretion rate inside the spherization radius can be approximated by the linear relation (compare solid and dotted curves in Fig. 1b)

$$\dot{m}(r) \approx \dot{m}_{\rm in} + (\dot{m}_0 - \dot{m}_{\rm in})\,\frac{r}{r_{\rm sp}}. \tag{25}$$

This can be easily understood from equation (12): the radial derivative of the accretion rate is proportional to $r^2Q(r)$, which is almost constant at $r < r_{\rm sp}$. The linear behaviour of the accretion rate on radius is also obtained in the numerical simulations (Ohsuga et al. 2005).

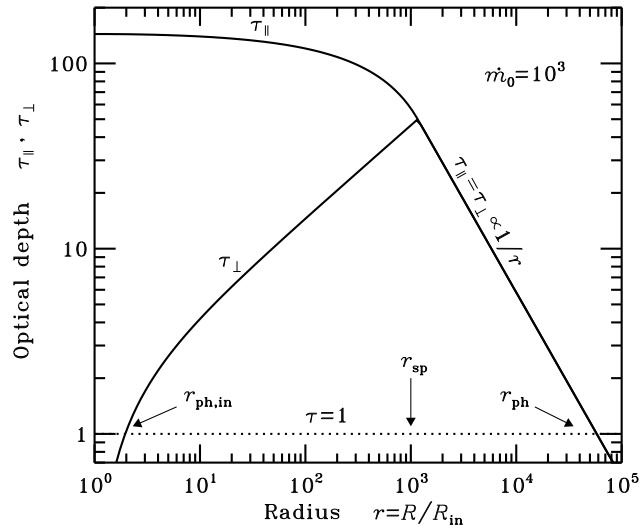

Figure 2. The Thomson optical depth through the wind as a function of radius in the direction parallel and perpendicular to the disc for $\dot{m}_0 = 10^3$. The wind parameters are $\beta = \zeta = 1$ and $\epsilon_{\rm w} = 1/2$. The perpendicular optical depth reaches the maximum of $\sim 3\dot{m}_0^{1/2}\frac{\epsilon_{\rm w}}{\beta} \sim 50$ at the spherization radius $r_{\rm sp} \approx \dot{m}_0$.

4 STRUCTURE OF THE OUTFLOW

4.1 Optical depth through the outflow

The gas ejected from the accretion disc at cylindrical radius R gains the velocity perpendicular to the disc (in the z direction), $v_z = \xi v_{\rm K}(R)$ with $\xi \gtrsim 1$. A mass element reaches asymptotically the velocity of $\zeta v_{\rm K}(R)$, with $\zeta = \sqrt{\xi^2 - 1}$. If the angular momentum is conserved, the gas moves (in the ballistic approximation) along the line $z/R = \zeta$ at large radii. The radial (i.e. projected to the disc plane) velocity is thus $\zeta v_{\rm K}(R)/\xi$. Because the disc scale-height $H/R \sim 0.6$ and ξ is not expected to exceed 1.5–2 (owing to the energy constraints), $\zeta \sim 0.6$–1.7. The outflow is thus confined in the region outside the cone of opening angle θ given by $\cot\theta = \zeta$ and it occupies $\Omega_{\rm w}/4\pi = \cos\theta = 0.5$–$0.85$ fraction of the sky.

Let us construct the vertically averaged wind model. As our baseline we take the advective disc model with the outflow described in the previous section. We take the accretion rate as given by equation (25) with $r_{\rm sp}$ and $\dot{m}_{\rm in}$ given by equations (21) and (23). The mass outflow rate (at $r < r_{\rm sp}$) is then

$$\dot{M}_{\rm w}(R) = \int_{R_{\rm in}}^{R} \frac{{\rm d}\dot{M}(R)}{{\rm d}R}{\rm d}R = \dot{M}_{\rm Edd}(\dot{m}_0 - \dot{m}_{\rm in})\frac{r-1}{r_{\rm sp}}. \quad (26)$$

Within the spherization radius the mean wind radial velocity should scale with the local Keplerian velocity. At $R > R_{\rm sp}$, the mass loss rate is constant and the gas reaches asymptotically velocity of $\sim \beta\, v_{\rm K}(R_{\rm sp})$, where $\beta \sim \zeta \sim 1$. We can then approximate the wind radial velocity profile by a simple function:

$$v_{\rm w}(R) = \begin{cases} \beta\sqrt{\frac{GM}{R}}, & R \le R_{\rm sp}, \\ \beta\sqrt{\frac{GM}{R_{\rm sp}}}, & R > R_{\rm sp}. \end{cases} \quad (27)$$

From the mass conservation law,

$$\dot{M}_{\rm w}(R) = \zeta\, 4\pi R^2\, \rho(R)\, v_{\rm w}, \quad (28)$$

we find the mean density ρ and the optical depth in the perpendicular direction, $\tau_\perp(R) = \kappa\rho\zeta R$:

$$\tau_\perp(r) = \frac{\tau_0}{\beta}\frac{\dot{m}_0 - \dot{m}_{\rm in}}{r_{\rm sp}} \begin{cases} r^{1/2} - r^{-1/2}, & r \le r_{\rm sp}, \\ (r_{\rm sp}-1)r_{\rm sp}^{1/2} r^{-1}, & r > r_{\rm sp}. \end{cases} \quad (29)$$

Here $\tau_0 = \dot{M}_{\rm Edd}\sqrt{6}\kappa/4\pi c R_{\rm in} \approx 5$. The optical depth has the maximum $\tau_{\perp,\max} \approx 3(\dot{m}_0^{1/2} - \dot{m}_0^{-1/2})\epsilon_{\rm w}/\beta$ at $r = r_{\rm sp}$ (see Fig. 2).

The Thomson optical depth from radius r in the direction parallel to the disc is

$$\tau_\parallel(r) = \kappa\int_R^\infty \rho(R'){\rm d}R' = \frac{1}{\zeta}\int_r^\infty \tau_\perp(r')\frac{{\rm d}r'}{r'}. \quad (30)$$

The maximum of $\sim 8(\dot{m}_0^{1/2} - 4/3)\epsilon_{\rm w}/\zeta\beta$ is reached at $r = 1$. At $r > r_{\rm sp}$ it decays in the way identical to $\tau_\perp$ (Fig. 2):

$$\tau_\parallel(r) = \tau_\perp(r)/\zeta \propto r^{-1}. \quad (31)$$

The outflow becomes optically thick at $\dot{m}_0 \sim 2.5$ for $\epsilon_{\rm w} \sim 1/2$.

4.2 Photospheres and the emitted spectrum

We can define three characteristic radii (see Fig. 2): (1) the radius of the inner photosphere $r_{\rm ph,in}$, where $\tau_\perp = 1$; (2) the spherization radius $r_{\rm sp} \approx \dot{m}_0$, where the optical depth through the wind in the normal direction is maximal; and (3) the outer photosphere $r_{\rm ph}$, where the wind becomes transparent $\tau_\perp \approx \tau_\parallel = 1$.

The inner photosphere is almost independent of $\dot{m}_0$:

$$r_{\rm ph,in} \approx 1 + \frac{\beta}{3\epsilon_{\rm w}}. \quad (32)$$

The outer photosphere (for $\dot{m}_0 \gg 1$),

$$r_{\rm ph} \approx 3\,\frac{\epsilon_{\rm w}}{\zeta\beta}\,\dot{m}_0^{3/2}, \quad (33)$$

is much larger than the spherization radius.

A face-on observer would see the emission from three separate zones defined by the three characteristic radii:

$$\begin{array}{ll} r < r_{\rm ph,in}, & \text{zone A}, \\ r_{\rm ph,in} < r < r_{\rm sp}, & \text{zone B}, \\ r_{\rm sp} < r < r_{\rm ph}, & \text{zone C}. \end{array} \quad (34)$$

The characteristic disc temperatures can be obtained from the Stefan-Boltzmann law

$$Q_{\rm rad}(R) = \sigma_{\rm SB}T^4(R). \quad (35)$$

For the advective disc with $\epsilon_{\rm w} = 1/2$ the maximum effective temperature is about

$$T_{\max} = 1.6\; m^{-1/4}\left(1 - 0.2\dot{m}_0^{-1/3}\right)\ {\rm keV}. \quad (36)$$

It is reached at $r_{\max} \approx 1.06 < r_{\rm ph,in}$ for large $\dot{m}_0$ and varies little with the accretion rate. Variations in $\epsilon_{\rm w}$ affects this temperature only by a per cent or so (see Fig. 1a). The observed color temperature differs from $T_{\max}$ by a color correction factor $f_{\rm c}$. The exact values for $T_{\max}$ and $r_{\max}$, however, depend on general relativity corrections, which are neglected here. In zone A, the wind is transparent (i.e. it is momentum-driven) and the radiation escapes unaffected by the outflow.

In zone B, the wind is opaque and the energy generated in the disc is advected by the wind. The ratio of the photon diffusion time in the wind, $\tau_\perp\zeta R/c$, to the dynamical time-scale, $\zeta R/v_{\rm w}$, is $3\epsilon_{\rm w}/\sqrt{6} \sim 1$ (this supports the view that the wind here is energy-driven). Thus the radiation escapes at a radius about twice the energy generation radius. This does not change the radial dependence of the effective temperature $T \propto R^{-1/2}$, resulting in a power-law

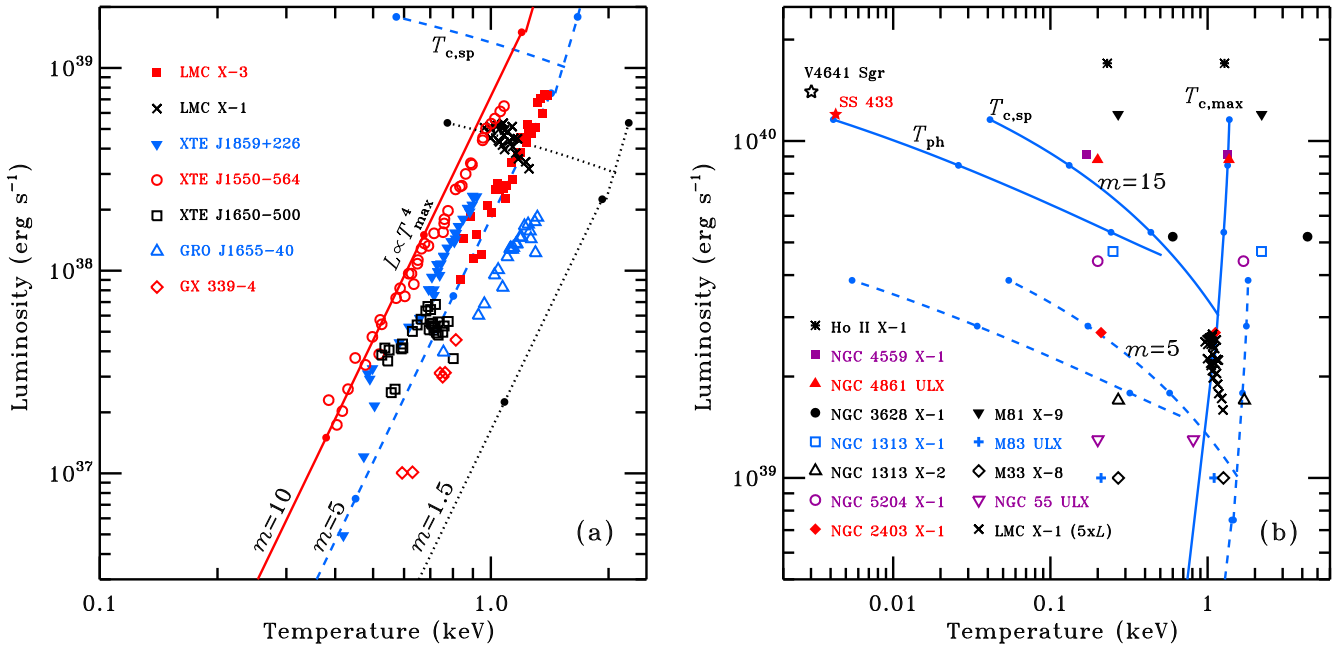

Figure 3. (a) The luminosity-temperature relation for sub-critically accreting BHs in the Milky Way and Large Magellanic Cloud (data from Gierliński & Done 2004). Most objects (except LMC X-1) show a well pronounced correlation $L \propto T^4_{\rm max}$ consistent with the standard accretion theory (SS73). The bolometric luminosity and the color temperature $T_{\rm c,max}$ are corrected here for the effect of inclination and relativistic effects (see details in Gierliński & Done 2004). Theoretical dependences are shown for 1.5, 5 and 10 solar mass BHs. (b) The luminosity-temperature relation for super-critically accreting BHs. The curves are theoretical dependences for the model of the advective disc with the outflow given by equations (19) and (36)–(38). The accretion rate is $\dot{m}_0 \approx 2$ at the point of separation of various temperatures, and the curves continue until $\dot{m}_0 = 10^3$ (filled circles at the curves indicate a change in $\dot{m}_0$ by a factor of 10). The following temperatures are shown (from the right curve to the left): the maximal color disc temperature $T_{\rm c,max} = f_{\rm c} T_{\rm max}$ with the color correction factor $f_{\rm c} = 1.7$, the color temperature at the spherization radius $T_{\rm c,sp}$ (also with $f_{\rm c} = 1.7$), and the temperature at the outer photosphere $T_{\rm ph}$. The wind parameters are $\beta = \zeta = 1$, $\epsilon_{\rm w} = 1/2$. The upper (solid) set of curves is for the BH mass $m = 15$ and the lower dashed curves are for $m = 5$. The stars show the positions of the super-critically accreting stellar-mass BHs, SS 433 (Dolan et al. 1997) and V4641 Sgr (Revnivtsev et al. 2002). Other symbols are the apparent bolometric luminosities and the temperatures obtained from the spectral fits with the blackbody and DISKBB model to the *XMM-Newton* data of a set of ULXs (from Table 5 of Stobbart et al. 2006). The crosses show the data for LMC X-1 if one increases the apparent luminosity by a factor of 5.

spectrum $F_E \propto E^{-1}$ extending from about $T_{\rm ph,in}$ to the temperature at the spherization radius $r_{\rm sp} \approx \dot{m}_0$:

$$T_{\rm sp} \approx 1.5\, m^{-1/4} \dot{m}_0^{-1/2} \left(1 + 0.3\, \dot{m}_0^{-3/4}\right) \ \text{keV}. \qquad (37)$$

The resulting temperature should also be reduced by $(1-\epsilon_{\rm w})^{1/4}$, because some energy is transferred to the outflow.

The outer zone C emits about the Eddington luminosity which is produced mostly in the disc at radii $r > r_{\rm sp}$. The photon diffusion time here is smaller than the dynamical time, thus most of the radiation escapes not far from the radius it is produced. This results in the effective temperature variation close to $r^{-3/4}$ and the nearly standard spectrum $F_E \propto E^{1/3}$ (SS73).

An edge-on observer would see only the blackbody-like emission corresponding to the temperature at the outer photosphere, which for $\dot{m}_0 \gg 1$ (i.e. $r_{\rm ph} \gg r_{\rm sp}$) takes the form:

$$T_{\rm ph} \approx 0.8 \left(\frac{\zeta\beta}{\epsilon_{\rm w}}\right)^{1/2} m^{-1/4} \dot{m}_0^{-3/4} \ \text{keV}. \qquad (38)$$

For accretion rates slightly exceeding the Eddington, $r_{\rm ph} \lesssim r_{\rm sp}$, and the dependence of $T_{\rm ph}$ on $\dot{m}_0$ is much stronger.

At intermediate inclinations, the central hot part of the disc may be partially blocked by the wind, and an observer would see a soft spectrum peaking at $T_{\rm sp}$.

5 COMPARISON WITH OBSERVATIONS

The standard model for sub-critically accreting BHs (SS73; Sect. 2) predicts the relation $L \propto T^4_{\rm max} \propto \dot{M}$. At super-Eddington accretion rates, three characteristic temperatures are identified: (i) the maximal color disc temperature $T_{\rm c,max} = f_{\rm c} T_{\rm max} \approx 1.6 f_{\rm c} m^{-1/4}$ keV, (ii) the color temperature at the spherization radius $T_{\rm c,sp} \approx 1.5 f_{\rm c} m^{-1/4} \dot{m}_0^{-1/2}$ keV, and (iii) the outer photosphere temperature given by equation (38). The bolometric luminosity and the temperatures depend parametrically on $\dot{m}_0$ according to equations (19) and (36)–(38). These theoretical dependences are shown in Fig. 3(b). The luminosity observed along the symmetry axis may exceed $L_{\rm bol}$ by a factor $1/(1-\cos\theta)$∼2–10 for the outflow height z/R∼0.6–2. On the other hand, a fraction $\epsilon_{\rm w}$ is spent on acceleration of the outflow. Together these effects result in the 10–30-fold excess over $L_{\rm Edd}$ at high accretion rates (see also Ohsuga et al. 2005; Begelman et al. 2006; Fabrika et al. 2006). Thus the absolute maximum apparent luminosity in our model is about 10^{41}erg s^{-1} for a 20 $\mathrm{M}_\odot$ BH.

The BHs in the Milky Way and LMC, accreting at a rate above a few per cent of Eddington, show spectra peaking at 0.4–1.5 keV. They closely follow the standard $L \propto T^4_{\rm max}$ dependence (except LMC X-1, see Gierliński & Done 2004, and Fig. 3a). The spread around it can result from varying contribution of the non-thermal emission. A shift of the microquasar GRO J1655-40 to the right from the L–T relation for a 7 $\mathrm{M}_\odot$ BH (Orosz & Bailyn 1997) is

probably related to a high spin of the BH there, which results in a higher disc temperature compared to the Schwarzschild BH.

Two super-Eddington accretors in our galaxy, a persistent source SS 433 (Dolan et al. 1997) and a super-critical transient V4641 Sgr (Revnivtsev et al. 2002), show optical spectra with characteristic temperatures of 30 000–50 000 K, which we associate with the emission from the outer photosphere (and not with the spherization temperature $T_{\rm sp}$ as proposed by Begelman et al. 2006). We estimate the accretion rate to be about 10^3 higher than the Eddington one. SS 433 is a bright UV source with total luminosity of about $10^{40}{\rm erg\ s^{-1}}$ (Dolan et al. 1997), but is underluminous in the X-rays. V4641 Sgr, on the other hand, exceeded 12 Crab in the X-rays during the outburst and and was extremely bright in the optical band. Such a difference may be caused by a different mode of accretion and/or different inclination of the two systems.

In Fig. 3(b) we present the data for ULXs with the luminosities exceeding $10^{39}{\rm erg\ s^{-1}}$ and the most reliable spectra obtained by *XMM-Newton*. The temperatures obtained by Stobbart et al. (2006) from the fits with the blackbody and DISKBB models and the corresponding observed bolometric luminosities are plotted. A theoretical spectrum from a super-critical disc with a $T(R) \propto R^{-1/2}$ dependence, can, in principle, be represented as a sum of such components. We associate a high temperature component with the hot inner disc of $T_{\rm max}{\sim}1$ keV. A high BH spin and an overheating of the disc above the effective temperature at $\dot{m}_0{\sim}2$–20 (Beloborodov 1998; Suleimanov et al. 2002; Kawaguchi 2003) may be responsible for sometimes observed higher (up to 4 keV) temperatures. A soft, $\sim$0.2 keV component may correspond to the spherization temperature implying the accretion rate $\dot{m}_0 = m^{-1/2}(1.5 f_{\rm c}/T_{\rm c,sp}[{\rm keV}])^2{\approx}30$–40 onto a stellar mass, 10–20 $\mathrm{M}_\odot$, BH. The observed higher luminosities can result from the geometrical beaming.

LMC X-1 deserves a more detailed discussion. Its apparent luminosity is sub-Eddington for a 10 $\mathrm{M}_\odot$ BH, but its track on the *L–T* diagram (see Fig. 3a) is perpendicular to that for other BHs. This can be understood if its mass is only $\sim 1.5\mathrm{M}_\odot$ (i.e. it can be a neutron star, but see Hutchings et al. 1983; Ebisawa et al. 1991) and the source accretes at $\dot{m}_0{\sim}3$. The observed rather soft spectrum is associated with the spherization region and results from obscuration of the central hot disc. In that case, however, we seriously underestimate the true luminosity of the object. Assuming that it is five time larger than the apparent one, the behaviour of LMC X-1 on the *L–T* plane (Fig. 3b) becomes consistent with that of the spherization temperature at $\dot{m}_0 {\approx}1$–3 for a 10 $\mathrm{M}_\odot$ BH.

6 SUMMARY

A black hole accreting at a super-Eddington rate is likely to produce strong winds (and jets) as observed in SS 433, the only known BH in the Milky Way accreting persistently at such a high rate. The bolometric luminosity can exceed the Eddington limit by a logarithmic factor $\sim \ln \dot{m}_0$, while the apparent luminosity can be factor of 5 higher because of the geometrical beaming. The observational appearance of such an object strongly depends on the inclination angle of the system to the line-of-sight. In edge-on systems, the central X-ray source is hidden by the wind and most of the radiation, with the characteristic temperature of $\sim 10^4$–10^5 K, escapes in the UV band. A face-on observer sees the hot inner flow with the flat in EF_E spectrum extending from a few keV down to the temperature at spherization radius $T_{\rm sp} \approx \dot{m}_0^{-1/2}$ keV.

Strong winds from the accretion disc explain naturally the presence around the ULXs of the expanding nebulae which are photoionized by the X-ray and UV radiation of the central source. An excellent agreement between the model and the data supports views (Fabrika & Mescheryakov 2001; King 2002; Fabrika 2004; Begelman et al. 2006; Vierdayanti et al. 2006) that ULXs are super-critically accreting stellar-mass BHs similar to SS 433, but observed along the symmetry axis.

ACKNOWLEDGEMENTS

This work was supported by the Academy of Finland grants 102181, 111720, 107943, 109122, 110792 and 112982, the Magnus Ehrnrooths Foundation, the Vilho, Yrjö and Kalle Väisälä Foundation, the Russian RFBR grants 04-02-16349 and 06-02-16025-a, and the RFBR/JSPC grant 05-02-19710. JP thanks the Kavli Institute for Particle Astrophysics and Cosmology and the Max-Planck-Institut für Astrophysik for hospitality during his visits. We thank Marek Gierliński for the data and Ramesh Narayan for valuable suggestions.

REFERENCES

Abolmasov P., Fabrika S., Sholukhova O., Afanasiev V., 2007, Astroph. Bull., 62, 36 (astro-ph/0612765)
Abramowicz M. A., Czerny B., Lasota J. P., Szuszkiewicz E., 1988, ApJ, 332, 646
Begelman M. C., Hatchett S. P., McKee C. F., Sarazin C. L., Arons J., 1980, ApJ, 238, 722
Begelman M. C., King A. R., Pringle J. E., 2006, MNRAS, 370, 399
Beloborodov A. M., 1998, MNRAS, 297, 739
Bisnovatyi-Kogan G. S., Blinnikov S. I., 1977, A&A, 59, 111
Blandford R. D., Begelman M. C., 1999, MNRAS, 303, L1
Colbert E. J. M., Mushotzky R. F., 1999, ApJ, 519, 89
Dewangan G. C., Griffiths R. E., Rao A. R., 2006, ApJ, 641, L125
Dolan J. F., et al. 1997, A&A, 327, 648
Ebisawa K., Mitsuda K., Hanawa T., 1991, ApJ, 367, 213
Eggum G. E., Coroniti F. V., Katz J. I., 1988, ApJ, 330, 142
Fabrika S., 2004, Astrophysics and Space Physics Reviews, 12, 1
Fabrika S., Abolmasov P., 2006, in Kissler-Patig M., Roth M. M., Walsh J. R., eds, ESO and Euro3D Workshop, Science Perspectives for 3D Spectroscopy, in press (astro-ph/0602364)
Fabrika S., Mescheryakov A., 2001, in Schilizzi R. T., Vogel S. N., Paresce F., Elvis M. S., eds, IAU Symp. 205, Galaxies and their Constituents at the Highest Angular Resolution. Astron. Soc. Pac., San Francisco, p. 268 (astro–ph/0103070)
Fabrika S., Karpov S., Abolmasov P., Sholukhova O., 2006, in Meurs E. J. A., Fabbiano G., eds, IAU Symp. 230, Populations of High Energy Sources in Galaxies. Cambridge University Press, Cambridge, p. 278 (astro–ph/0510491)
Feng H., Kaaret P., 2007, ApJ, submitted
Fukue J., 2004, PASJ, 56, 569
Gierliński M., Done C., 2004, MNRAS, 347, 885
Hutchings J. B., Crampton D., Cowley A. P., 1983, ApJ, 275, L43
Jaroszyński M., Abramowicz M. A., Paczyński B., 1980, Acta Astronomica, 30, 1
Kaaret P., Corbel S., Prestwich A. H., Zezas A., 2003, Sci, 299, 365
Kaaret P., Ward M. J., Zezas A., 2004, MNRAS, 351, L83
Katz J. I., 1986, Comm. Astrophys., 11, 201

Kawaguchi T., 2003, ApJ, 593, 69
King A. R., 2002, MNRAS, 335, L13
King A. R., Pounds K. A., 2003, MNRAS, 345, 657
King A. R., Davies M. B., Ward M. J., Fabbiano G., Elvis M., 2001, ApJ, 552, L109
Kitabatake E., Fukue J., Matsumoto K., 2002, PASJ, 54, 235
Körding E., Falcke H., Markoff S., 2002, A&A, 382, L13
Lehmann I., et al. 2005, A&A, 431, 847
Lipunova G. V., 1999, Astron. Lett., 25, 508
Makishima K., et al. 2000, ApJ, 535, 632
Miller J. M., Fabbiano G., Miller M. C., Fabian A. C., 2003, ApJ, 585, L37
Miller J. M., Fabian A. C., Miller M. C., 2004, ApJ, 614, L117
Morgan E. H., Remillard R. A., Greiner J., 1997, ApJ, 482, 993
Mushotzky R., 2004, Prog. Theor. Phys. Suppl., 155, 27
Narayan R., Yi I., 1994, ApJ, 428, L13
Ohsuga K., Mori M., Nakamoto T., Mineshige S., 2005, ApJ, 628, 368
Okuda T., Teresi V., Toscano E., Molteni D., 2005, MNRAS, 357, 295
Orosz J. A., Bailyn C. D., 1997, ApJ, 477, 876
Pakull M. W., Mirioni L., 2003, in Jansen F., ed, ESA SP-488: New visions of the X-ray Universe in the XMM-Newton and Chandra era. ESA, Noordwijk (astro–ph/0202488)
Pakull M. W., Grisé F., Motch C., 2006, in Meurs E. J. A., Fabbiano G., eds, IAU Symp. 230, Populations of High Energy Sources in Galaxies. Cambridge University Press, Cambridge, p. 293 (astro–ph/0603771)
Ramsey C. J., Williams R. M., Gruendl R. A., Chen, C.-H. R., Chu Y.-H., Wang Q. D., 2006, ApJ, 641, 241
Revnivtsev M., Gilfanov M., Churazov E., Sunyaev R., 2002, A&A, 391, 1013
Reynolds C. S., et al. 1997, MNRAS, 286, 349
Shakura N. I., Sunyaev R. A., 1973, A&A, 24, 337 (SS73)
Shimura T., Takahara F., 1995, ApJ, 445, 780
Stobbart A.-M., Roberts T. P., Wilms J., 2006, MNRAS, 368, 397
Strohmayer T. E., Mushotzky R. F., 2003, ApJ, 586, L61
Strohmayer T. E., Mushotzky R. F., Winter L., Soria R., Uttley P., Croppe M., 2007, ApJ, in press (astro-ph/0701390)
Suleimanov V. F., Ghosh K. K., Austin R. A., Ramsey B. D., 2002, Astronomy Letters, 28, 745
Vierdayanti K., Mineshige S., Ebisawa K., Kawaguchi T., 2006, PASJ, 58, 915
Vikhlinin A., et al. 1994, ApJ, 424, 395
Wang Q. D., 2002, MNRAS, 332, 764
Watarai K.-y., Fukue J., 1999, PASJ, 51, 725
Watarai K.-y., Fukue J., Takeuchi M., Mineshige S., 2000, PASJ, 52, 133
Zdziarski A. A., Johnson W. N., Poutanen J., Magdziarz P., Gierlinski M., 1997, in Winkler C., Courvoisier T. J.-L., Durouchoux P., eds, ESA SP-382: The Transparent Universe. p. 373